Journal of Welding Technology
P-ISSN: 2716-1471 | E-ISSN: 2716-0475
http://e-jurnal.pnl.ac.id/Welding_Technology

Comparative analysis on metallography, hardness, and corrosion rate of repair methods in welding tube SA-213 to tubesheet SA-240

Moh. Syaiful Amri*, Alvalo Toto Wibowo, Muh. Ofirsyah Apriliano Ananda Dzikrilla
Department of Welding Engineering, Shipbuilding Institute of Polytechnic Surabaya, Surabaya 60111, Indonesia
*Corresponding author: amri@ppns.ac.id

Article Processing Dates:
Received 2025-09-09
Accepted 2025-10-06
Available online 2025-12-31

Keywords:
Repair Welding
Tube to Tubesheet
Hardness
Metalography
Corrosion Rate

Abstract

In the fabrication process of heat exchangers, tube-to-tubesheet weld joints are often prone to defects such as porosity, cracking, undercut, and other forms of damage that can degrade the quality and performance of the equipment. To address these issues, repair becomes a crucial solution. However, due to the lack of standardized repair procedures, alternative methods such as TIG dressing and flush and reweld using filler metals of various diameters are commonly applied for the sake of time and cost efficiency. This study aims to compare three repair methods TIG dressing, flush and reweld using diameters 1.6 mm filler, and diameters 2 mm filler on macrostructure, microstructure, hardness, and corrosion rate of tube-to-tubesheet weld joints. The tests conducted include macro and micro examinations, Vickers Hardness testing, and corrosion rate. The results showed that Repair 1 (TIG dressing) produced a finer ferrite phase in the weld metal area and achieved the highest average Hardness value of 234.4 kgf/mm², although it also exhibited the highest corrosion rate at 0.44053 mm/year. In contrast, Repair 2 showed the lowest Hardness in the weld metal area, with an average of 221.9 kgf/mm², and the lowest corrosion rate of 0.28036 mm/year. Therefore, the TIG dressing method proves to be more effective in improving Hardness, but at the expense of an increased corrosion rate.

1. Introduction

The oil, gas, and power generation sectors, in particular, are under tremendous pressure to consistently increase efficiency and dependability due to the rapid growth of technology. One of the critical components supporting these industrial operations is the heat exchanger. A heat exchanger is a heat transfer device that transfers energy between two or more fluids at different temperatures, where the fluids are separated by a heat transfer surface to prevent mixing. This device plays a crucial role in various applications, such as in power generation, oil and gas, transportation, cooling, cryogenic, and heat recovery industries. Examples of its applications include car radiators, condensers, evaporators, air preheaters, and coolers. [1]

Heat exchanger manufacturing process, procedures that refer to applicable standards or codes, such as ASME and TEMA, are required. ASME (American Society of Mechanical Engineers) and TEMA (Tubular Exchanger Manufacturers Association) are codes and standards that are widely used in the industry to ensure the quality and safety of manufactured heat exchanger units [2]. These standards provide comprehensive guidelines, including aspects of design, materials, fabrication, and testing, as well as technical guidance throughout the heat exchanger fabrication process. In the heat exchanger fabrication process, precision in the welding process plays a crucial role. Due to mechanisms such as welding defects and the like, cracks and damage can easily form at the tube-to-tubesheet weld joints[3].

The most frequent problems in tube-to-tubesheet welding are flaws such undercuts, cracks, and porosity. This often results in high costs for replacing the affected material. In such cases, welding repair becomes the preferred option to address defects and reduce production costs[4]. However, owners often instruct that repairs be performed by replacing the defective tube before re-welding the tubesheet. This process involves removing the welded section (flushing) and then performing repair welding with a new tube. In terms of efficiency, this method is time-consuming and requires higher costs for tube replacement.

Due to the absence of standardized repair procedures, field fabrication teams often resort to using the TIG dressing repair method, which is more efficient in terms of time and cost without requiring tube replacement. In some cases, defects are repaired by removing the weld cap (flushing) and rewelding with added filler metal. To expedite the repair process, filler metal with a larger diameter is also frequently used [5].

The repair method chosen will affect the microstructure, mechanical properties, and corrosion rate of the material, especially when the product is applied to fluids that require good corrosion resistance. Therefore, this study will examine three repair methods: TIG dressing, flush and reweld with filler metal ø1.6 and ø2 mm. It is hoped that this study can provide information regarding the impact of repair methods on microstructure, hardness, and corrosion rate in tube-to-tubesheet welding. This information can serve as a consideration in selecting repair methods for similar projects[6].

This research focuses on comparing three repair methods for welding SA-213 TP304L tubes to SA-240 TP304L tubesheets in terms of metallography, hardness, and corrosion rate. The objective of this study is to determine how each repair method affects the microstructural characteristics, mechanical strength through hardness values, and durability through corrosion resistance. The study is expected to provide several benefits: for students, it enhances knowledge and allows practical application of welding engineering skills; for companies, it serves as a valuable reference in selecting effective repair methods to achieve high-quality results; and for the general public, it offers insights and literature on repair practices in heat exchanger

tube-to-tubesheet welding, contributing to better understanding and guidance in industrial applications.

2. Research Methods

2.1 Materials and Equipment

This study requires equipment and materials to support its implementation. Several materials are required to support this research. The materials required are as follows: (a). SA-213 TP304L tube material, (b). SA-240 TP304L tubesheet material, (c). ER 308L electrodes with diameters of 1.6 mm and 2 mm, (d). Ultra-high-purity argon gas (99.97%), (e). Sandpaper, (e). Tissue, (f). Etching solution (HCl + HNO_3) and (g). Alcohol

This research utilizes various supporting equipment in the processes of manufacturing, forming, testing, and analyzing test specimens to ensure optimal results. The equipment used includes the following types, (a). Gas Tungsten Arc Welding (GTAW) machine, (b). Vickers hardness tester, (c). Diamond pyramid indentor, (d). Grinding machine, (e). Facing tool, (f). Polishing machine, (g). Expanding tool, (h). Stopwatch, (i). Ampere clamp, (j). Hand dryer, (k). Beaker, (l). Personal Protective Equipment (PPE)

2.2 Welding Process

The tube-to-tubesheet welding process in this study used a GTAW (Gas Tungsten Arc Welding) welding machine with predetermined parameters and joint designs. The joint was then assumed to be defective, and three different repair processes were performed: Repair A (repair by TIG dressing), Repair B (repair by flush & reweld with filler metal 1.6 mm), and Repair C (repair by flush & reweld with filler metal 2 mm). The GTAW welding machine is shown in Fig. 1, and the parameter of welding as shown in Table. 1.

Fig. 1. GTAW Welding Machine

Table 1. Welding Parameters

Weld Layer	*Classification Filler metal*	Diameter *Filler metal*	*Travel speed* (mm/min)	*Amperage (range)*	*Voltage (Range)*	*polarity*
Root	ER 308L	1,6 mm	65-75	90-110	10-13	DC /SP
Fill/ Cap	ER 308L	1,6 mm	36-44	90-110	10-13	DC /SP

The welding procedure steps are as follows: (a). Clean the tube and tubesheet materials before fit-up, (b). Perform fit-up according to the prepared joint design, (c). Ensure the specimen is at room temperature (20–25°C) before welding, (d). Set the shielding gas flow rate at 10–16 L/min, (e). Adjust the welding current and voltage according to the parameters, (f). Carry out welding for the four existing joints, (g). Ensure the temperature remains below 150°C during the welding process and, (h). Allow the weld metal to cool down slowly, (see Fig. 2).

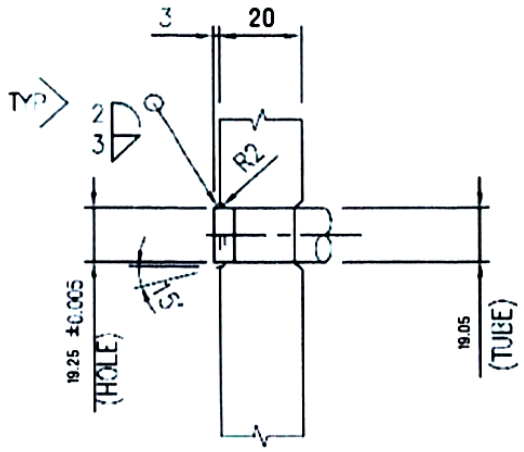

Fig. 2. Design Joint

The steps for Welding with Repair Technique 1 (Repair by TIG Dressing): **(a).** Clean the surface of the specimen to be repaired, (b). Ensure the specimen is at room temperature, around 20–25°C, before the repair process, (c). Make sure the tungsten tip is sharp to focus on the remelting area, (d). Set the shielding gas flow rate to 10–16 L/min, (e). Adjust the welding machine to a current range of 90–110 A and a voltage range of 10–13 V, (f). Perform the repair process using the TIG dressing method, (g). Maintain the tungsten distance at about 1–3 mm from the surface to ensure arc stability and uniform penetration (h). Ensure the temperature remains below 150°C during the repair process. (i). Allow the weld metal to cool slowly.

Repair Process 2

The steps for Welding with Repair Technique 2 (Repair by Flush and Reweld with Filler Metal): (a). Clean the surface of the specimen to be repaired, (b). Perform grinding to remove the weld capping, (c). Ensure the specimen is at room temperature, around 20–25°C, before the repair process, (d). Set the shielding gas flow rate to 10–16 L/min, (e). Adjust the welding machine to a current range of 90–110 A and a voltage range of 10–13 V, (f). Perform the repair process using filler metal with a diameter of ø1.6 mm, (g). Ensure the temperature remains below 150°C during the repair process, (h). Allow the weld metal to cool slowly.

Repair Process 3

Steps for Welding with Repair Technique 3 (Repair by Flush and Reweld with Filler Metal): (a). Clean the surface of the specimen to be repaired, (b). Perform grinding to remove the weld capping. (c). Ensure the specimen is at room temperature, around 20–25°C, before the repair process, (d). Set the shielding gas flow rate to 10–16 L/min, (e). Adjust the welding machine to a current range of 90–110 A and a voltage range of 10–13 V, (f). Perform the repair process

using filler metal with a diameter of ø2 mm, (g). Ensure the temperature remains below 150°C during the repair process, (h). Allow the weld metal to cool slowly.

2.3 Expanding Process

The tube expanding process for tube-to-tubesheet welded joints involves several steps to ensure proper expansion and joint integrity. The procedure begins with cleaning the tube and tubesheet surfaces, followed by dimensional inspection of the tube, holes, and tolerances. A roller expander with torque control is used to achieve uniform expansion and to maintain wall thickness reduction, which is targeted at 5% for stainless steel material. The expander is inserted into the tube, activated with the preset torque, and verified through measurements on initial samples to confirm that the wall reduction meets the required target, with adjustments made if necessary. After expansion, tubes are inspected for cracks or excessive deformation, and the inside diameter is checked to ensure it falls within the theoretical post-expansion criteria with a tolerance of 0.05 mm. Finally, the tubes are cleaned of any burrs resulting from the process. The actual parameters of the expansion process, including hole diameter, wall thickness, expansion ratio, inside diameter before and after expansion, and remarks on amperage.[7][8]

2.4 Penetrant Test

The penetrant testing process for tube-to-tubesheet welds begins with thorough surface preparation, ensuring the test area is clean, dry, and free from contaminants that may obstruct defect detection. During testing, both the material and penetrant must be maintained at room temperature (20–50°C), with the penetrant applied by brushing and left for a dwell time of around 5 minutes, with reapplication allowed to keep the surface wet. A thin, uniform layer of developer is then sprayed from about 25 cm after shaking the can, and observations are carried out under visible light of at least 1000 lux. Indications are interpreted within 10–30 minutes after the developer dries, and post-cleaning is performed immediately after testing to avoid component damage. The welds are evaluated based on [9] Div. 1 Appendix 8 acceptance criteria, which require the surface to be free from linear relevant indications longer than 1.5 mm, rounded relevant indications larger than 5 mm, or clusters of four or more rounded indications aligned with spacing ≤ 1.5 mm.

2.5 Specimen Preparation

Preparation of test specimens by cutting the entire specimen into several parts for metallographic, hardness, and corrosion rate testing. According to ASME IX, macro examination of tube-to-tubesheet welds requires cutting through the tube center, with specimen codes A (without repair), B (repair 1 by TIG dressing), C (repair 2 with 1.6 mm filler), and D (repair 3 with 2 mm filler) in Fig. 3

Fig. 3. Test Specimen

Metallography tests, both macro and micro, were conducted to evaluate the weld metal, heat-affected zone (HAZ), and base metal by surface preparation, grinding, polishing, etching, and microscopic observation. Hardness testing was performed using the Vickers method with a 1 kgf load to measure resistance to indentation across different weld regions. Meanwhile, corrosion rate testing was carried out electrochemically using a 3.5% NaCl solution to simulate seawater, with measurements obtained through potentiodynamic polarization to determine corrosion behavior of the weld surfaces. Corrosion rate measurement using a three-electrode cell electrochemical test refers to ASTM G5 (Standard Reference Test Method for Making Potentiodynamic Anodic Polarization Measurement) [10] with a test scheme as shown in Fig. 5 below. The advantage of this method is that we can immediately determine the corrosion rate when measured, so the measurement time does not take long time. To calculate the corrosion rate using the three-electrode cell electrochemical method, in Eq. 1, as follows.

The locations of the hardness testing points in each area are shown in Fig. 4.

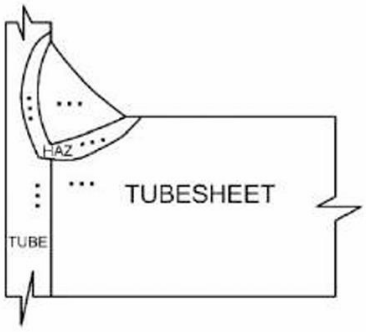

Fig. 4. Hardness test point

$$CR = \frac{K1\,.\,i\,cor\,.\,EW}{P} \quad \text{.....1}$$

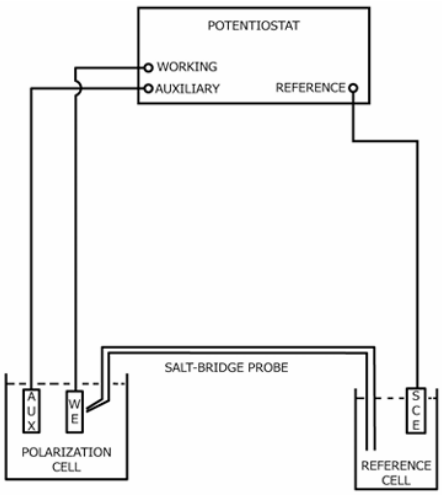

Fig. 5. Corrosion rate test scheme [10]

2.6 Data Analysis

At this stage, analysis and discussion were conducted on the results of the research, namely data on the comparison of repair methods in welding SA-213 TP304L tubes to SA 240 TP304L tubesheets in terms of microstructure, macrostructure, hardness values, and corrosion rates. After testing and obtaining the test results, the next step is to analyze the data to determine whether there is a significant effect that can be compared between the repair methods used. This data analysis uses the one-way ANOVA method with SPSS software.

3. Results and Discussion.

3.1 Results

Preparation and welding processes have been carried out. This subchapter will present the results of welding parameters, penetrant testing, macrostructure testing, microstructure testing, hardness testing, and corrosion rate testing as follows, see Table 2.

Welding parameters

Table 2. Welding Parameters

Parameter Pengelasan						
Spesimen	Layer	Amperage (A)	Voltage (V)	Flowrate (l/min)	Travel Speed (mm/min)	Heat Input (kj/mm)
A	1	106	10,4	10	65,36	1,012
	2	102	11	10	35,33	1,923
B	1	102	11,1	10	70,01	0,970
	2	105	10,5	10	36.54	1,810
C	1	105	10,5	10	66,55	0,994
	2	104	10,6	10	37,34	1,771
D	1	106	10,3	10	70,04	0,935
	2	104	10,1	10	39,1	1,632

The parameters during the welding repair process on specimens with repair 1 (TIG dressing), repair 2 (flush & re-weld with 1.6 mm filler), and repair C (flush & re-weld with 2 mm filler) in Table 3.

Table 3. Welding Repair Parameters

Parameter *Repair*						
Repair	*Layer*	*Amperage (A)*	*Voltage (V)*	*Flowrate (l/min)*	*Travel Speed (mm/min)*	*Heat Input (kj/mm)*
1	2	98	10,1	10	35,45	1,675
2	2	102	10,1	10	41,45	1,491
3	2	111	10,2	10	49,35	1,377

Penetrant test results

Liquid dye penetrant testing is a non-destructive test to find discontinuities in the surface of the test specimen based on the principle of capillarity[11]. Documentation of the results of the liquid dye penetrant test in Fig. 6.

Fig. 6. Penetrant test result

From Fig. 6, that the welding process on the tube-to-tubesheet joint complies with the acceptance criteria for liquid penetrant in ASME VII DIV 1 APPENDIX 8 [12]. Therefore, the specimen can be said to meet the acceptance criteria, meaning that the welding process has passed the penetrant test and can proceed to the next process without any repeat repairs. This success is due to the welding parameters used not deviating from the qualified WPS.

Macrostructure

Macro structure testing was carried out with the aim of finding out whether the material or test specimen used in this study produced good quality in each specimen from the welding process that had been carried out in each variation, which is shown in Fig.s 7, 8, 9, and 10.

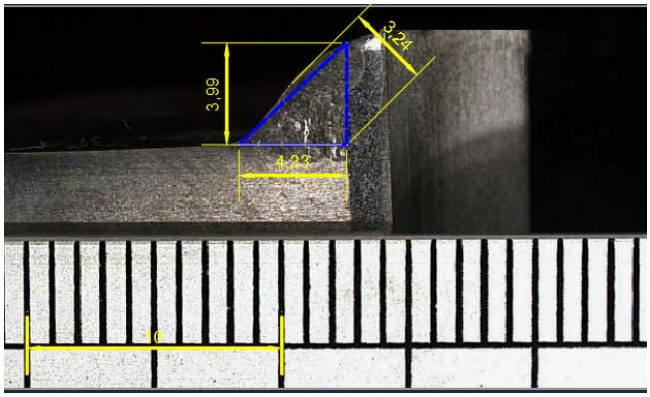

Fig. 7. spesimen test without repair

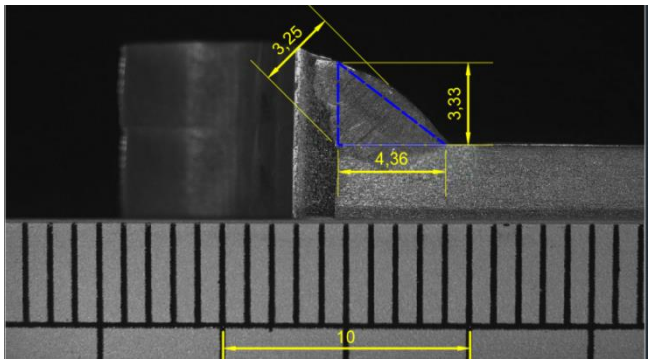

Fig. 8. repair by TIG dressing

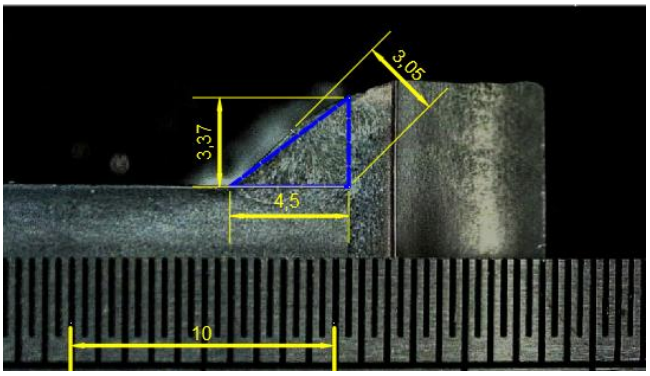

Fig. 9. Repair by flush & reweld with filler 1,6 mm

F

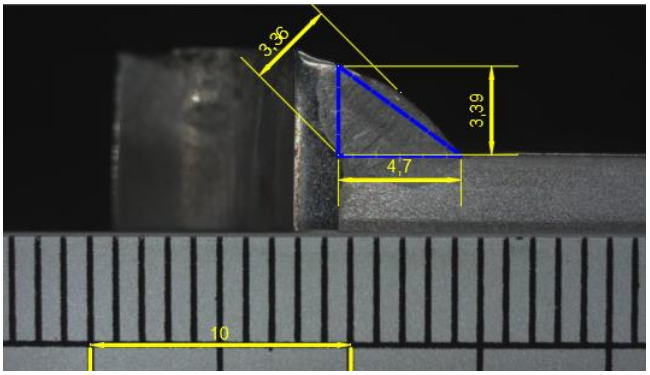

Fig. 10. Repair by flush and reweld with filler 2 mm.

Macrostructure testing of the tube-to-tubesheet welds showed complete fusion, indicating that the welding parameters used were in accordance with the WPS. Measurements of leg length and weld throat obtained through AutoCAD confirmed compliance with the *Heat Exchanger Design Handbook* requirement of 1.4 × tube thickness, with vertical–horizontal leg length differences below 3 mm, meeting ASME Section IX acceptance criteria. Dilution analysis revealed values of 25.30% for the specimen without repair (a), 27.91% for TIG dressing repair (b), 38.48% for flush & reweld with 1.6 mm filler (c), and 36.20% for flush & reweld with 2 mm filler (d). The highest dilution occurred in specimen (c), with specimens (c) and (d) showing similar results due to both involving filler addition, while TIG dressing resulted in lower dilution because it was performed without filler.

Microstructure

During micro testing, images were taken of the base metal, HAZ, and weld metal. This micro testing was conducted using 200x magnification to see in more detail the microstructure formed after the welding and repair process. *without repair* (a), *repair by* TIG *dressing* (b), *repair* by *flush* & *reweld with filler* 1,6 mm. (c), *repair* by *flush* & *reweld with filler* 2 mm. (d) as shown in Fig. 11, 12, 13, 14 and 15.

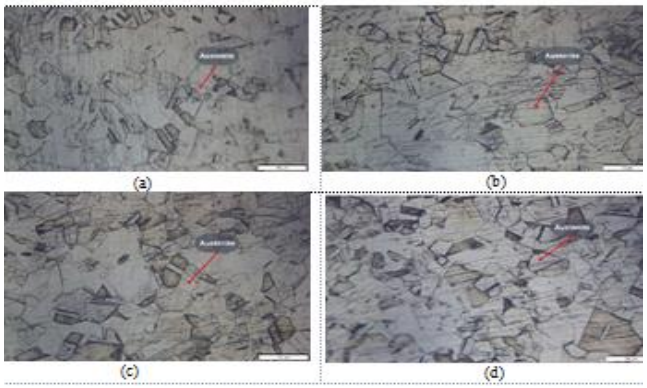

Fig. 11. Results of Micro Base Metal Tube Testing

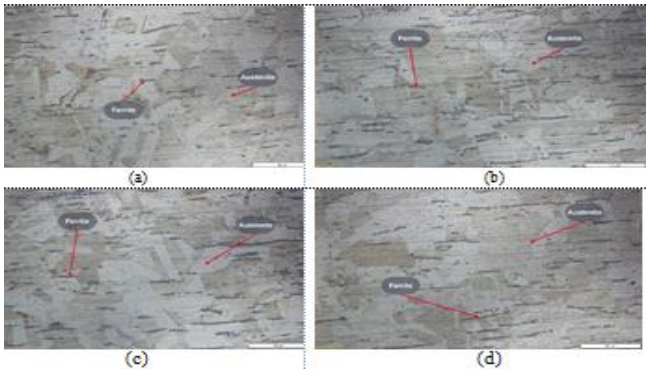

Fig. 12. Base Metal Tube Micro Test Results

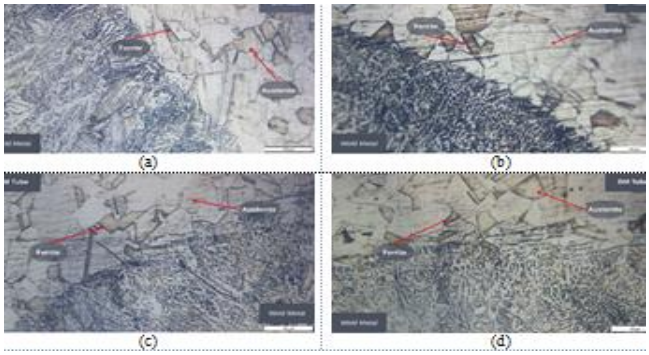

Fig. 13. HAZ Tube Micro Test Results

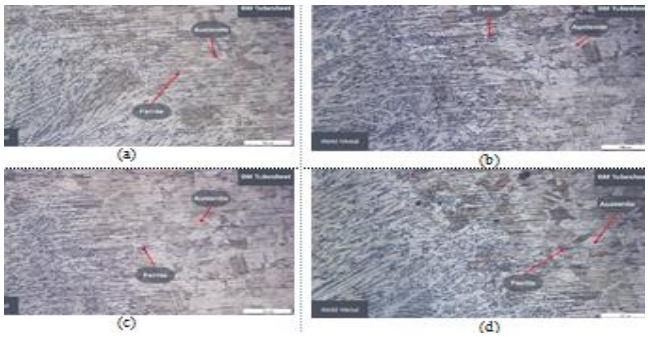

Fig. 14. Microstructure of Tubsesheet HAZ

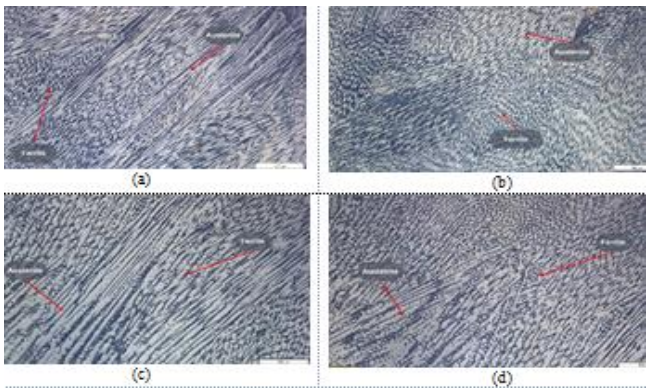

Fig. 15. Microstructure of Weld Metal

The microstructural analysis of tube-to-tubesheet welds on 304L stainless steel showed consistent phases across different regions and repair methods. In the base metal of both tube and tubesheet, the dominant phase was austenite with secondary ferrite appearing along grain boundaries, while differences in thermal conductivity influenced grain growth—faster cooling in the thinner tube limited ferrite growth, whereas slower cooling in the thicker tubesheet promoted coarser grains and deeper ferrite penetration into the fusion zone. The HAZ of both tube and tubesheet exhibited similar austenite–ferrite structures, with the tubesheet HAZ showing higher hardness due to coarser ferrite growth from slower cooling. In the weld metal, all specimens contained austenite with skeletal delta ferrite, though TIG-dressed repairs produced finer ferrite morphology, which correlates with higher hardness[13]. The presence of delta ferrite is beneficial in preventing solidification cracking, but excessive amounts can reduce ductility, toughness, and corrosion resistance.

Hardness

Hardness testing was conducted using the Vickers method (kgf/mm²) with a load of 1 kgf for 10 seconds. The locations of indentations in the BM, WM, and HAZ regions of each variation and their results in Fig. 16.

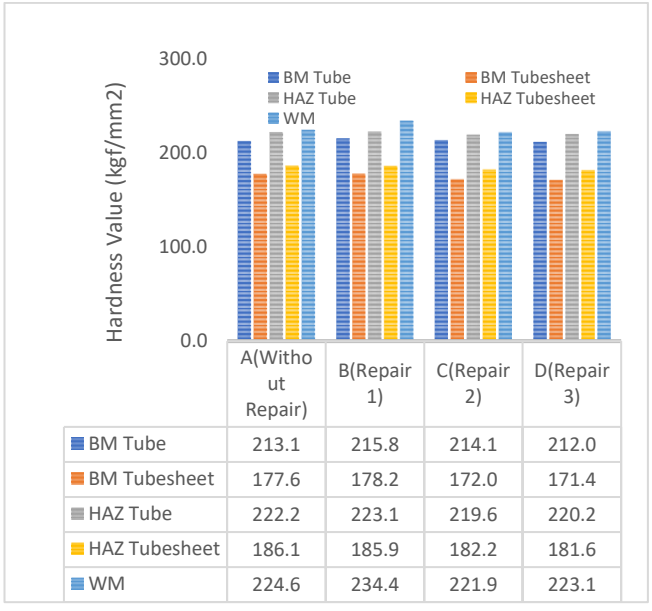

	A(Without Repair)	B(Repair 1)	C(Repair 2)	D(Repair 3)
BM Tube	213.1	215.8	214.1	212.0
BM Tubesheet	177.6	178.2	172.0	171.4
HAZ Tube	222.2	223.1	219.6	220.2
HAZ Tubesheet	186.1	185.9	182.2	181.6
WM	224.6	234.4	221.9	223.1

Fig. 16. Hardness Test Chart

The hardness test results for tube-to-tubesheet welds showed variation across different regions, with the highest values generally observed in specimens repaired by TIG dressing (B), particularly in the base metal tube (215.8 kgf/mm²), base metal tubesheet (178.2 kgf/mm²), HAZ tube (223.1 kgf/mm²), and weld metal (234.4 kgf/mm²). In contrast, the lowest hardness values were mostly found in specimens repaired by flush & reweld with filler 2 mm (D), while the HAZ tubesheet recorded its highest hardness in the unrepaired specimen (A).

One-way ANOVA analysis

The statistical analysis began with a normality test using the Anderson-Darling method, which showed that all P-values were greater than the significance level ($\alpha = 0.05$), indicating that the data were normally distributed. A homogeneity test using Levene's method was then conducted, and the results confirmed that all samples had homogeneous variances, as P-values were also greater than 0.05. With both assumptions satisfied, a one-way ANOVA was performed to assess the effect of different repair methods on hardness values. The results revealed no significant effect on the HAZ tube and HAZ tubesheet regions, as their P-values exceeded 0.05, while a significant effect was observed in the weld metal region, where the P-value was less than 0.05.

Corrosion rate

Corrosion rate testing was conducted to evaluate the effect of various welding repair methods using a 3.5% NaCl solution (pH 6.8) to simulate seawater conditions. Six specimens were tested, including base metal pipe (BMTU), base metal sheet pipe (BMTS), without repair (A), and three repaired specimens (B, C, D). The results in Fig. 17.

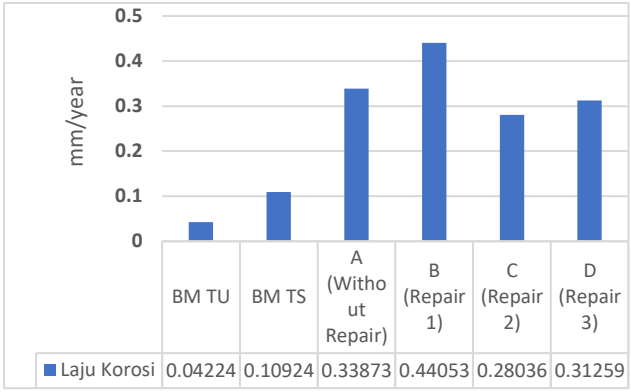

Fig. 17. Corrosion Rate Chart

The potentiodynamic polarization curves were analyzed using Tafel extrapolation to determine corrosion current density (Icorr) and corrosion potential (Ecorr), which were then used to calculate corrosion rates. Results showed that base metals had the lowest corrosion rates (0.04224 mm/year for tube and 0.10924 mm/year for tubesheet), while welded specimens exhibited higher rates. Among the repaired samples, the TIG dressing repair (B) showed the highest corrosion rate (0.44053 mm/year), whereas flush & reweld with filler 1.6 mm (C) had the lowest (0.28036 mm/year). These findings indicate that welding and repair processes significantly increase corrosion susceptibility, particularly in the knife zone near the weld, where chromium carbide

precipitation reduces the protective passive layer and accelerates localized corrosion[14].

3.2 Discussion

The present research focuses on an experimental study analyzing the effectiveness of three repair methods for tube-to-tubesheet weld joints, namely TIG dressing, flush & reweld with 1.6 mm filler, and flush & reweld with 2 mm filler. To evaluate the performance of these repair techniques, several testing procedures were applied, including liquid dye penetrant, metallographic observation, hardness measurements, and corrosion rate analysis. The liquid penetrant inspection revealed that all specimens successfully met the acceptance requirements of ASME Section IX (2023), confirming that the welds were free from surface-breaking defects and suitable for further examination. This initial result indicated that the welding quality of the repaired joints was sufficient to undergo more detailed structural and mechanical characterization.

The macrostructural examination further showed that all specimens exhibited smooth weld deposits, free from macroscopic defects such as porosity, cracks, or lack of fusion. The weld throat height complied with the recommendation of the Heat Exchanger Design Handbook [1], which specifies 1.4 times the tube thickness, while the dimensional tolerance between vertical and horizontal leg lengths was below 3 mm. These findings confirm that the weld geometry conformed to international standards. Dilution analysis revealed the highest dilution ratio in specimen C (38.48%), followed closely by specimen D, as both involved filler addition after removing the weld cap. Specimen A, repaired with TIG dressing, showed a lower dilution of 27.91% since no filler was applied. Such variations in dilution significantly influence the metallurgical bonding at the fusion line and potentially affect mechanical and corrosion performance [15].

Microstructural analysis of the base metal tube, made of SA 213 type 304L stainless steel, revealed a predominantly austenitic structure with minor ferrite distributed along grain boundaries. Similarly, the base metal tubesheet also exhibited austenitic dominance with stringer-like ferrite appearing as a secondary phase. These results are consistent with the description provided by [16], who explained that austenitic stainless steels of type 304L may present either a fully austenitic structure or a mixture of austenite with ferrite stringers. The tube region, due to its thinner wall and higher thermal conductivity, experienced rapid heat dissipation during welding, leading to finer ferrite formation. In contrast, the thicker tubesheet displayed slower cooling, resulting in coarser ferrite growth into the fusion zone. This finding highlights how thermal conductivity and material thickness govern solidification behavior during welding[17].

Further analysis of the weld metal microstructure showed that it was dominated by elongated austenite with skeletal delta ferrite. Among the specimens, repair 1 (TIG dressing) produced a finer ferrite distribution compared to the other methods, which is advantageous in improving mechanical strength. The presence of delta ferrite is generally associated with enhanced hardness due to its stronger lattice structure compared to austenite, but excessive ferrite content may compromise ductility, toughness, and corrosion resistance. [18] noted that controlling ferrite content in stainless steel welds is crucial to balancing mechanical and corrosion properties. Thus, while TIG dressing provided a refined ferrite structure, it also raised concerns regarding possible corrosion susceptibility in the long term.

Hardness testing confirmed these microstructural findings. The base metal tube exhibited values between 212.0–215.8 Kgf/mm², which were attributed to cold working during the tube expansion process after welding. The tubesheet recorded values between 171.4–178.2 Kgf/mm², showing little variation since stainless steel is non-heat-treatable and relatively stable in hardness. The HAZ of the tube presented slightly higher hardness, with the highest value recorded in specimen B (223.1 kgf/mm²). Notably, the weld metal itself displayed the highest hardness in specimen B, averaging 234.4 Kgf/mm², which is consistent with the presence of more refined ferrite. According to [19], an increase in delta ferrite content correlates with higher hardness, though at the expense of ductility. Importantly, all hardness values remained within the permissible limit of 250 HV specified for stainless steel in the Heat Exchanger Design Handbook [1], confirming the suitability of all repair methods from a mechanical strength perspective.

The corrosion test provided a different perspective on repair performance. The base metal tube showed the lowest corrosion rate at 0.04224 mm/year, while the tubesheet followed with 0.10924 mm/year. The unrepaired specimen displayed a higher rate of 0.33873 mm/year, reflecting the influence of welding on corrosion behavior. Among repaired specimens, TIG dressing exhibited the highest corrosion rate at 0.44053 mm/year, whereas flush & reweld with 1.6 mm filler achieved the lowest rate of 0.28036 mm/year. Corrosion was predominantly observed in the knife zone, the thin region between the weld metal and the HAZ, where chromium carbide ($Cr_{23}C_6$) precipitation at grain boundaries disrupts passive film stability. As explained by [14], this phenomenon reduces corrosion resistance locally, even when the bulk stainless steel material remains resistant. These findings indicate that although TIG dressing improves hardness, it compromises corrosion performance more than the other methods.

From the overall results, a trade-off is evident between hardness and corrosion resistance. The increase in hardness achieved through TIG dressing also coincides with an increase in corrosion rate. This relationship is consistent with the findings of [20], who emphasized that although finer ferrite phases may enhance hardness, they do not always improve corrosion resistance. Thus, repair method selection should be tailored to operational requirements. TIG dressing is recommended when mechanical strength and resistance to deformation are prioritized, while flush & reweld with 1.6 mm filler is more suitable for applications requiring better long-term corrosion resistance. Ultimately, determining the optimal repair technique depends on whether the heat exchanger will operate under conditions where strength or corrosion performance is the primary concern.

4. Conclusions.

This study concluded that all three repair methods produced a defect-free macrostructure with excellent fusion, while microstructural analysis indicated austenite as the dominant phase and ferrite as a secondary phase. Specifically, TIG dressing (Repair 1) resulted in finer ferrite in the weld metal

compared to the coarser ferrite distribution in Repairs 2 and 3, which directly affected hardness. Hardness testing revealed that fewer repair treatments resulted in higher hardness values, especially in the weld metal region. However, corrosion testing showed that TIG dressing (Repair 1) resulted in the highest corrosion rate compared to Repairs 2 and 3, indicating that a finer ferrite phase may increase corrosion susceptibility. For future research, it is recommended to use finite element analysis to study the effects of residual stresses, explore multiple repair cycles for greater insight, and test alternative filler materials to optimize performance.

References

[1] T. Kuppan, *Heat exchanger design handbook*. CRC Press, 2013.

[2] Thakur A. N. C. P., P. P. Thakur, "A Review on Effects of GTAW Process Parameters on weld," 2017, doi: doi: 10.13140/RG.2.2.11535.38569.

[3] C. M. L. W. L. Liu, N. Ding, J. Shi, N. Xu, W. Guo, "Failure analysis of tube-to-tubesheet welded joints in a shell-tube heat exchanger," *Case Stud Eng Fail Anal*, vol. 7, pp. 32–40, 2016, doi: doi: 10.1016/j.csefa.2016.06.002.

[4] Barzegar-Mohammadi R. M. S., M. Haghpanahi, M. Zeinoddini, "Cooling rate effects on fatigue life prediction using hardness measurements for in-service steel patch-welds with and without TIG dressing treatment," *Structures*, vol. 50, pp. 1285–1302, 2023, doi: doi: 10.1016/j.istruc.2023.02.019.

[5] I. D. AghaAli, M. Farzam, M. A. Golozar, "The effect of repeated repair welding on mechanical and corrosion properties of stainless steel 316L," *Mater Des*, vol. 54, 2014, doi: doi: 10.1016/j.matdes.2013.08.052.

[6] K. O. L. H. J. Yi, Y. J. Lee, "Tig dressing effects on weld pores and pore cracking of titanium weldments," *Met.*, vol. 6, no. 10, 2016, doi: doi: 10.3390/met6100243.

[7] TEMA 11th, "Standards of the Tubular Exchanger Manufacturers Association 8th Edition," *TEMA - Tubul. Exch. Manuf. Assoc.*, p. 298, 2023.

[8] D. T. Thekkuden, A. H. I. Mourad, T. Ramachandran, A. H. Bouzid, R. Kumar, and A. Alzamly, "Combined effect of tungsten inert gas welding and roller expansion processes on mechanical and metallurgical characteristics of heat exchanger tube-To-Tubesheet joints," *J. Mater. Res. Technol.*, vol. 21, pp. 4724–4744, 2022, doi: 10.1016/j.jmrt.2022.11.043.

[9] ASME IX, "Qualification Standard for Welding, Brazing, and Fusing Procedures; Welders; Brazers; and Welding, Brazing, and Fusing Operators SECTION IX Welding, Brazing, and Fusing Qualifications 2023 ASME Boiler and Pressure Vessel Code An International Code," in *www.asme.org/cer*, 2023.

[10] ASTM G5, *Reference Test Method for Making Potentiodynamic Anodic Polarization Measurements*. ASTM International, 2021. doi: https://doi.org/10.1520/G0005-14R21.

[11] H. B. K. M.M Munir, M. Thoriq Wahyudi, *MODUL PRAKTIK DT NDT*. 2024.

[12] ASME VIII, *RULES FOR CONSTRUCTION OF PRESSURE VESSELS*. 2023.

[13] M. F. Saffiudeen *et al.*, "Combined Gas Tungsten Arc Welding and Shielded Metal Arc Welding Processes for Joining Tube to Tubesheet in Shell and Tube Heat Exchangers," *J. Press. Vessel Technol. Trans. ASME*, vol. 146, no. 4, 2024, doi: 10.1115/1.4065519.

[14] Mohammed. H. A. A. G. R., M. Ishak, S. N. Aqida, "Effects of heat input on microstructure, corrosion and mechanical characteristics of welded austenitic and duplex stainless steels: A review," *MDPI AG*, no. Feb. 01, 2017, doi: doi: 10.3390/met7020039.

[15] Vaghani A. K. D. M., S. A. Vasanwala, "Stainless Steel As A Structural Material: State Of Review," *www.ijera.com*, 2014.

[16] J. C. Lippold and D. J. Kotecki, *WELDING METALLURGY AND WELDABILITY OF STAINLESS STEELS*. 2005.

[17] Hassan. M. R. E.-K., Ahmed, Iman El-Mahallawi, "Effect of GTAW Welding Current on the Quality of 304L Austenitic Stainless Steel Using ER316L."," *Int. J. Mater. Technol. Innov.*, 2023, doi: 10.21608/ijmti.2023.190981.1075.

[18] S. Kou, *Welding Metallurgy*, vol. 4, no. 3. 2003. doi: 10.22486/iwj.v4i3.150243.

[19] Ghasemi M. F.-N. R. Ghasemi, B. Beidokhti, "Effect of delta ferrite on the mechanical properties of dissimilar ferritic-austenitic stainless steel welds," *Arch. Metall. Mater.*, vol. 63, no. 1, pp. 437–443, 2018, doi: doi: 10.24425/118958.

[20] G. Palumbo et al, "Effect of grain size on the corrosion behavior of Fe-3wt.%Si-1wt.%Al electrical steels in pure water saturated with CO2," *Materials (Basel).*, vol. 14, no. 17, p. doi: 10.3390/ma14175084, 2021.